Supercritical Fluid Tuning of Reactions Rates: the Cis−Trans Isomerization of 4-4′-Disubstituted Azobenzenes

Angela K. Dillow,† James S. Brown, Charles L. Liotta, and Charles A. Eckert*

Schools of Chemical Engineering and Chemistry and Specialty Separations Center, Georgia Institute of Technology, Atlanta, Georgia 30332-0100

Received: March 25, 1998; In Final Form: June 26, 1998

Remarkable tuning of reaction rates has been achieved for the isomerization of several dye molecules in supercritical fluid solvents using both small pressure changes and small additions of cosolvents. Rates of the thermal cis−trans relaxation were measured spectroscopically following irradiation for three dyes in supercritical carbon dioxide and ethane, pure and with several polar and protic cosolvents. The results are explained in terms of local density and composition enhancements, as well as by a change of mechanism due to strong hydrogen bonding. This study demonstrates the versatility of supercritical fluid solvents both to examine reaction mechanisms and as a means to tune rates.

Introduction

A remarkable range of tunability is one of the enormous advantages of supercritical fluid (SCF) solvents as reaction media. Not only do small pressure variations give large density changes with concomitant changes in solvent power, but SCFs can be further tailored with the addition of small amounts of cosolvents selected for their specific intermolecular interactions. Here we demonstrate the tuning of the rate of the thermal cis−trans isomerization of 4-(diethylamino)-4′-nitroazobenzene (DENAB) and some related compounds in SCF solutions.

Azobenzene compounds have been of both mechanistic and practical importance; many applications stem from their special push−pull properties.[1,2] The strong charge-transfer process resulting from the electron-donating and electron-withdrawing groups of the disubstituted azobenzenes produce strong absorption bands in the visible region, and consequently represent a large group of dyes.[3] Polymers impregnated with push−pull azobenzenes have been commonly used as molecular probes, triggers, and liquid crystals, and for nonlinear optics.[4,5] The reversible, photoinduced isomerization of these push−pull azobenzenes is the rate-limiting step of the trans/cis cycle used in reversible optical storage.[4−6]

Although the thermal cis−trans isomerization follows first-order kinetics in solution,[1−7] the mechanism of this isomerization is still disputed in polar or protic (hydrogen bond donating (HBD)) solvents. The kinetics of this isomerization in polymeric environments would be more accessible if the mechanism of isomerization in a variety of solvent environments were determined unequivocally.

While unsubstituted or push−push azobenzenes generally isomerize through an inversion mechanism,[8−11] debate still exists concerning the isomerization mechanism of push−pull azobenzenes such as 4-(dialkylamino)-4′-nitroazobenzenes. In nonpolar, aprotic (non-HBD) solvents, it is generally agreed that the isomerization of this class of compounds proceeds through an inversion mechanism characterized by an isopolar transition state (see Figure 1). However, the isomerization in polar and/or protic solvents, where the large solvent effects could stabilize a highly dipolar transition state, is thought to proceed through a rotation mechanism after the rupture of the azo double bond (see Figure 1).

One side of the debate argues that the isomerization reaction for 4-(dialkylamino)-4′-nitroazobenzene proceeds by inversion in all solvents,[11] based on the following studies:

1. Both push−push and push−pull reaction rate constants correlate with Taft polarity−polarizability parameters, where the solvent dipole/solvent-induced dipole have equal importance on the push−push and push−pull azobenzenes and this is responsible for the sizable solvent effects.[12]

2. Another investigator justifies the solvent effects through coplanar resonance structures of the transition state.[13] However, in this same work it was reported that for a series of 4′-(diethylamino)-nitroazobenzenes in DMF, a Hammet type plot of log k versus σ^+ and σ^- produced two distinct linear regions with ρ values of −3.25 and 10.2. This normally would be a clear indication of a change in mechanism, but the authors claimed the experimental data were evidence for the inversion mechanism in all cases.

3. Similar kinetic behavior between push−pull and other types of azobenzenes suggests that the single mechanism is inversion.[14]

4. A study of 15 "bipolarity" azobenzenes (none of which were 4-(dialkylamino)-4′-nitroazobenzenes) reports no dependence of the rate constants on the solvent order.[11]

Other evidence supports isomerization via a rotation mechanism in highly dielectric or protic solvents.,[1,15−19] Here the two mechanisms compete; the inversion mechanism will dominate in nonpolar, aprotic solvents, which could not effectively solvate the highly dipolar transition state of rotation mechanism. Such a hypothesis is consistent with the near-zero activation volume observed in nonpolar solvents such as hexane.[8] However, when protic or polar solvents are used, large negative activation volumes (−25.9 mL/mol in chloroform, −29.6 mL/mol in acetone) suggest a change in mechanism to rotation through a highly polar transition state stabilized by solvation.[8] Additionally, Kirkwood-type plots indicate strong

* Corresponding author.
† Present address: Department of Chemical Engineering and Materials Science, University of Minnesota, Minneapolis, MN.

S1089-5639(98)01634-X CCC: $15.00
Published on Web 09/09/1998

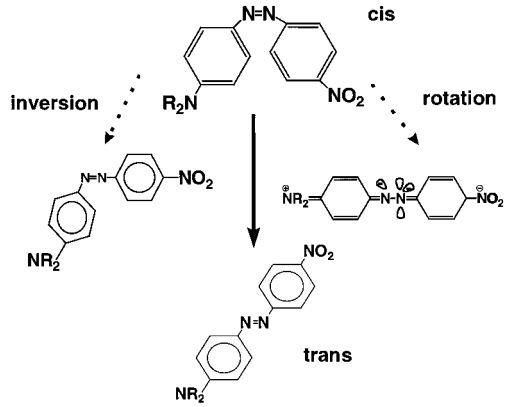

Figure 1. Isomerization by inversion mechanism (isopolar transition state) and rotation (dipolar transition state).

TABLE 1: SCF Solvents and Reaction Conditions for Each Solvent

SCF	density range (mol/L)	dielectric range
carbon dioxide (CO_2)	7−19	1.2−1.5
ethane (C_2H_6)	6−13	1.2−1.5

positive deviations from linearity at large values of the dielectric constant, additional evidence for a change in mechanism (i.e., from inversion to rotation).[8]

Whitten and co-workers[1] contend that the rate enhancement for polar, aprotic solvents is due to stabilization of the transition state by dielectric effects. However, specific interactions between the protic solvent and the hydrogen bond accepting (HBA) nitro group provides additional stabilization of the transition state when protic solvents are used, enhancing the charge transfer within the molecule.

Leffler and Sigman used the variable, density-dependent properties of SCF carbon dioxide (CO_2) to try to determine the mechanism of isomerization of 4-(diethylamino)-4′-nitroazobenzene (DENAB).[19] Although the density, viscosity, and diffusivity of SCF CO_2 change dramatically in the near-critical region,[20] the dielectric constant and π^* (Kamlet−Taft polarity/polarizability solvent parameter) vary only modestly. Therefore, determining mechanistic changes in a single solvent through adjustable, density-dependent properties was not possible. However, the CO_2 rate data were used along with the data from several nonpolar and polar liquid studies to generate a plot of $\Delta G^{\ddagger}$ (Gibb's energy of activation) versus π^*. This plot revealed two linear regions: the liquid alkanes and SCF CO_2 formed one line with a small, positive slope, while the liquid polar solvents formed a second line with a large, negative slope. The difference in value of these slopes suggests a change in mechanism from inversion to rotation.

Supercritical fluids have solvent properties between those of gases and liquids − near liquid-like densities (and corresponding solubilizing power) and diffusivities and viscosities which approach those in gases. In the near-critical region, these properties are a strong function of density, and large changes in solvent properties can be obtained with very small changes in pressure. For some SCFs (e.g., SCF CO_2 and SCF ethane) the dielectric constant changes only modestly as a function of density (see Table 1).

Even more profound tunability is achieved with the addition of small amounts of specifically chosen cosolvents (typically 1−5 mol %). Cosolvents can enhance solubility in supercritical fluids by orders of magnitude through specific interactions coupled with local composition enhancements.[21−27] Also reaction rates may be tuned in this near-critical region due to changes in solvent properties. The high compressibility leads to large, negative solute partial molar volumes, which may give large negative activation volumes. Local composition enhancements of a cosolvent about the reactant(s) further affect the rate in this highly compressible region.[28−35]

TABLE 2: Molecular Structures of Azo Reactants

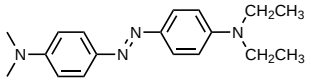

4-(diethylamino)-4′-nitroazobenzene (DENAB)

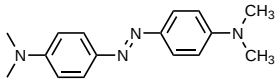

4-(dimethylamino)-4′-nitroazobenzene (DMNAB)

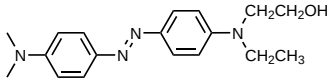

Disperse Red (DR)

TABLE 3: Cosolvent Structures and Properties

cosolvent	α^a	β^a	π^a	ϵ
methanol (CH_3OH)	0.93	0.62	0.6	32.7[d]
1,1,1,3,3,3-hexafluoro-2-propanol ($CF_3CH(OH)CF_3$)	1.96	0.00	0.65	16.6[b]
acetone (CH_3COCH_3)	0.08	0.48	0.71	20.7[c]
dimethylacetamide ($CH_3CON(CH_3)_2$)	0.00	0.76	0.88	37.8[e]

[a] Reference 58. [b] Reference 59. [c] Reference 18. [d] Reference 8. [e] Reference 60.

The purpose of this work is 2-fold—determination of the kinetics and mechanism and a demonstration of solvent tuning in SCFs. First, the reaction kinetics of the thermal cis−trans isomerization of a series of push−pull 4-(diethylamino)-4′-nitroazobenzenenes in pure SCFs ethane and CO_2 are determined. Reactant structures are given in Table 2. Ethane does not interact specifically with the solutes and exhibits little change in solvent dielectric with density; therefore, the effects of pressure can be isolated. Supercritical CO_2 also has little change in solvent dielectric with density, but may engage in specific interactions with the solutes.[36]

Second, through the use of small amounts of specifically chosen cosolvents (1 mol % and less), we may vary solvent properties substantially. Cosolvents used in this experiment and their properties are shown in Table 3. Through the use of polar/aprotic and polar/protic cosolvents, the effects of polarity/hydrogen-bonding ability (i.e., specific interactions) may be separated, and the effect on reaction kinetics will aid in the definition of reaction mechanism. Since the small amount of cosolvent affects the (low) SCF bulk dielectric constant very little, the effect of hydrogen bonding on the reaction rate is also separable.

Experimental Section

Materials. The materials used are listed in Table 4. The 4-(diethylamino)-4′-nitroazobenzene (DENAB) was synthesized as described elsewhere[19] and was recrystallized from toluene 3 times. The disperse red (DR) was also recrystallized from toluene 3 times. NMR spectra confirmed the structure of these compounds. All other materials were used as received. All cosolvents were used as received.

Apparatus. A schematic of the modified UV−vis diode array spectrophotometer (Hewlett-Packard 8453) is shown in Figure 2. The spectrophotometer was modified to accommodate a stainless steel high-pressure cell with 3 quartz windows

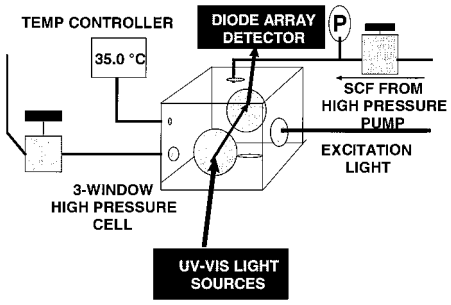

Figure 2. Schematic of experimental apparatus.

TABLE 4: Materials, Sources, and Purities

compound	source	purity (%)
4-(diethylamino)-4′-nitroazobenzenenitroazobenzene	synthesized	
4-(dimethylamino)-4′-nitroazobenzene	Aldrich Rare Chemical Library	
Disperse Red	Aldrich	99
carbon dioxide	Matheson, SCF Grade	99.99+
ethane	Matheson, C. P. Grade	99.9+
methanol	Aldrich, HPLC Grade	99.9+
acetone	Aldrich, HPLC Grade	99.9+
dimethylacetamide	Aldrich, HPLC Grade	99.9+
1,1,1,3,3,3-hexafluoro-2-propanol	Aldrich	99+

(Heraeus Amersil). The path length of the cell was 3 cm and the volume was 19.3 ± 0.15 mL. The windows were sealed with indium.[37] The cell was stirred continuously using a mini stir plate (Variomag) and a Teflon-coated stir bar (Fisher) placed inside the cell.

The cell temperature was monitored with an internal thermocouple and an external thermocouple within the steel block (Omega, type K, calibrated within ±0.1 °C) The cell was controlled by a PID controller (Omega) and backup heat was supplied constantly using an EPSCO DC power supply (Model D-612T) with thermoelectric Peltier heaters (Melcor). The pressure was controlled using either a 60 cm^3 piston type high-pressure generator (High Pressure Equipment, Model 87-6-5) or a high-pressure syringe pump (ISCO, 500D) and measured to within ±2 psi with a Heise digital pressure gauge (Model 901B). A Valco 6-port sampling valve with external sample loops ranging in size from 50 to 100 μL was used to inject cosolvent directly into the high-pressure cell. Visible light used to induce photoisomerization was supplied by a 500 W tungsten light passed through a UV filter.

Kinetic Measurements. Single-beam diode array spectroscopy was used to monitor absorbance as a function of increasing pressure at constant probe and cosolvent concentrations. Samples were irradiated with visible light for approximately 1 min, time-based absorbance measurements by the UV−vis diode array were initiated, the light was then blocked by a shutter (to give and accurate zero time), and the relaxation of the trans isomer to the cis isomer was monitored. Reaction rates were independent of irradiation time (after a minimum time) and independent of the percent reactant isomerized to the cis form, as was reported previously.[13]

The absorbance was recorded at the wavelength of maximum absorption for the trans isomer, where the change in absorbance is a maximum and where the contribution from the cis isomer is negligible for DENAB and DMNAB.[1,12,16,19] The rate constants were calculated from the absorbance measurements, assuming Beer's law. The absorbance was measured at two additional wavelengths to ensure that the contributions to the rate constant from the absorbance of the cis isomer were

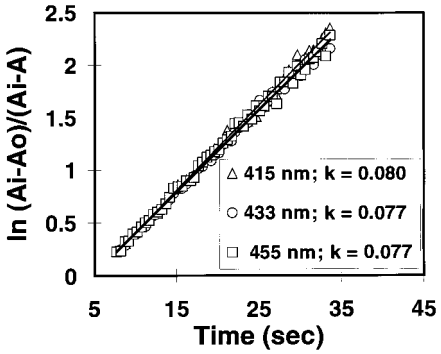

Figure 3. $\ln(A - A_\infty/A_0 - A_\infty)$ vs time (slope = rate constant (1/s)). DENAB in SCF CO_2. T = 35.6 °C.

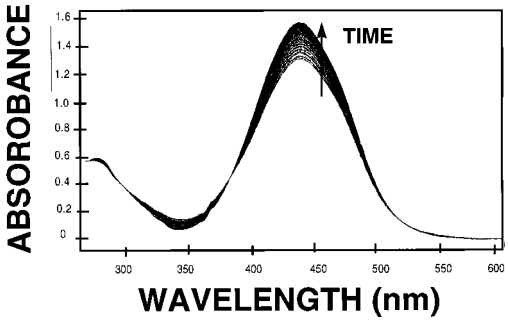

Figure 4. Sample time-based spectra of DENAB in SCF CO_2 modified with 0.056 M DMA. P = 158 bar, T = 35 °C.

negligible. The rates calculated from the changes in absorbance were measured at 415, 433, and 455 nm simultaneously for DENAB in SCF CO_2 are shown in Figure 3; rate constants calculated from all wavelengths are well within experimental error. Errors resulting from monitoring the absorption of DR at the wavelength of maximum absorption for the trans form would be negligible since only 3−5% of the compound was photoisomerized to the cis form in each decay experiment. This was verified by comparing the measurements of the rate of isomerization from both the wavelength of maximum absorption of the cis and trans isomers; the rate constants agreed within experimental error. Because the change in absorbance was much greater for the trans isomer, the errors associated with the rate constant measured at this wavelength were much smaller, and rate constants reported are based on measurements at this wavelength of maximum absorbance.

Two to seven time-based absorbance spectra were obtained at every pressure point. Sample time-based spectra, representative of the time-based spectra throughout this experiment, are shown in Figure 4.

Sample Preparation. All measurements were made at a constant temperature of 35 °C (±0.1 °C) and were carried out in the single-phase region, as confirmed by separate miscibility experiments.[38−41] Time-based spectra were obtained, starting at low pressures and incrementally going to higher pressures. The pressure varied less than 1 psi within a single spectral scan, and data sets were taken with increasing pressure to ensure that the solute concentration remained constant.

The high-pressure cell was loaded with a solution of solute dissolved in acetone using a micrometering pipet to obtain a probe concentration below the solubility limit at experimental conditions as determined spectroscopically. Experimental solute concentrations are given in Table 5. The cell was flushed with multiple volumes of low-pressure SCF solvent to evaporate the acetone and to displace air from the system. In the experiments with pure SCF solvents the cell was then pressurized with SCF

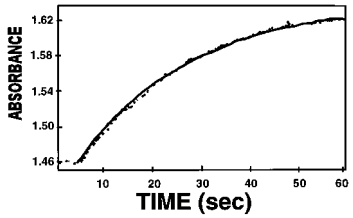

Figure 5. Fit of experimental absorbance data to a first-order exponential decay model for DENAB in SCF CO_2 modified with 0.126 M MeOH. $P = 155$ bar, $T = 35$ °C.

TABLE 5: Solute Concentrations

solute	concentration (M)
DENAB	1.4×10^{-5}
DMNAB	1.5×10^{-5}
Disperse Red	1.35×10^{-5}

TABLE 6: Experimental Cosolvent Compositions

SCF	cosolvent	conc (M)	mol %
ethane	MeOH	0.128	0.97−1.48
ethane	HFIP	0.049	0.25−0.3
ethane	acetone	0.07	0.54−0.86
ethane	DMA	0.056	0.43−0.63
CO_2	MeOH	0.064	0.35−0.45
CO_2	MeOH	0.128	0.67−1.1
CO_2	HFIP	0.025	0.13−0.25
CO_2	HFIP	0.049	0.27−0.36
CO_2	DMA	0.056	0.58−0.9

to the desired initial pressure. In cases where cosolvent was added, the cell was charged with 100 psig of SCF after removing air from the system. The cell was then isolated from the rest of the system, and the lines leading to the cell were pressurized with 450 psig of SCF. The external sample loop was then rinsed and filled with the cosolvent, and the sampling valve and the valve leading to the cell were opened simultaneously to force the cosolvent into the cell using the pressure differential. The cell was further pressurized with SCF to the desired pressure set point, and after equilibration of temperature and pressure, absorbance spectra were measured as described above. Concentrations and mole percents of cosolvents used for the various SCF solvents are given in Table 6.

Blank runs (no azobenzene) were made for each experiment to ensure that cosolvent was injected properly and that no contaminants were present. Replicate experiments with and without cosolvent resulted in rate constants within experimental error, ensuring that the method of cosolvent injection and experimental procedure were reproducible.

Data Analysis. All experiments followed first-order kinetics, and the rate constants were obtained by a fit of the time-based absorbance data to an exponential model (see Figure 5).

Since the azobenzene reactants were very dilute, mixture densities for the systems with no added cosolvent were assumed to be equal to the pure SCF density, calculated from the Benedict−Webb−Rubin (BWR) EOS. For the cosolvent-modified SCF mixture densities, we calculated the ratio of mixture density to pure SCF density from the Peng−Robinson (PR) EOS,[42] and used this ratio to correct the pure SCF density calculated from the BWR EOS. The mixture densities calculated by this method are reasonably accurate when less than 1 mol % cosolvent is used as determined by comparison with measured SCF/cosolvent mixture density data obtained in a separate experiment.[38] Critical properties and acentric factors used in the PR EOS calculations are listed in Table 7.

TABLE 7: Critical Properties and Acentric Factors Used for PR EOS[61]

compound	T_C (K)	P_C (bar)	ω
carbon dioxide	304.1	73.8	0.225
ethane	305.4	48.8	0.099
acetone	508.1	47.0	0.304
dimethylacetamide[a]	655.7	42.11	0.147
methanol	512.6	80.9	0.556
1,1,1,3,3,3-hexafluoro-2-propanol[a]	461.6	37.3	0.66

[a] Reference 62.

TABLE 8: Rate Constants for Cis to Trans Thermal Relaxation of DENAB in SCF Ethane and SCF Ethane Cosolvent Modified Solvents at 35 °C[a]

density (mol/L)	k (1/s)	density (mol/L)	k (1/s)
DENAB/Pure Ethane			
8.94	0.115	11.49	0.070
9.50	0.103	11.98	0.062
10.25	0.080	12.48	0.058
10.51	0.078	13.00	0.051
10.98	0.072		
DENAB/0.128 M MeOH			
8.63	0.154	10.83	0.105
8.82	0.134	11.14	0.106
9.62	0.136	11.46	0.093
9.83	0.126	11.97	0.084
10.11	0.121	12.26	0.075
10.36	0.122	12.74	0.064
10.54	0.117	13.14	0.057
DENAB/0.056 M DMA			
8.86	0.158	10.58	0.113
9.07	0.122	10.91	0.104
9.31	0.119	11.27	0.098
9.62	0.112	11.68	0.088
9.82	0.124	12.21	0.080
10.09	0.116	12.58	0.071
10.30	0.113	13.08	0.063
DENAB/0.049 M HFIP			
11.68	0.490	12.56	0.524
12.10	0.499	13.04	0.449
DENAB/0.07 M Acetone			
8.25	0.126	10.82	0.088
8.41	0.131	11.22	0.095
8.55	0.113	11.69	0.085
9.60	0.116	12.13	0.075
9.88	0.110	12.57	0.074
10.16	0.095	13.07	0.063
10.56	0.088		

[a] The uncertainty of the data is ±5%.

Results and Discussion

Rate constants were obtained for

(1) DENAB in SCF ethane; (2) DENAB, DMNAB, and DR in SCF CO_2; (3) DENAB in SCF ethane modified with cosolvents acetone, dimethylacetamide (DMA), methanol (MeOH), and 1,1,1,3,3,3-hexafluoro-2-propanol (HFIP); (4) DENAB, DMNAB, and DR in SCF CO_2 modified with DMA, MeOH, and HFIP.

The rate constants as a function of density are listed in Tables 8−12. There were no significant differences in the isomerization rates for DENAB, DMNAB, and DR in the pure SCF solvents; therefore DENAB was chosen as the focus solute for this work and the subsequent work with cosolvents because it exhibited the greatest solubility at low solvent densities in pure SCF solvents.

Reaction Rates of DENAB in Pure SCF CO_2 Pure SCF Ethane. The rate constant of the thermal cis−trans relaxation of DENAB in both pure SCF CO_2 and SCF ethane decreased

TABLE 9: Rate Constants for Cis to Trans Thermal Relaxation of DENAB in SCF CO_2 and Cosolvent-Modified Solvents at 35 °C[a]

density (mol/L)	*k* (1/s)	density (mol/L)	*k* (1/s)
DENAB/PURE CO_2			
9.1	0.123	14.5	0.058
9.9	0.104	15.1	0.052
10.5	0.099	16.1	0.046
12.4	0.076	17.1	0.038
13.5	0.071	18	0.032
DENAB/0.025 M HFIP			
10.06	0.298	13.79	0.165
10.56	0.253	14.48	0.137
11.43	0.220	15.29	0.128
11.78	0.202	16.17	0.113
12.19	0.190	17.22	0.099
12.37	0.187	18.18	0.085
12.76	0.176	18.81	0.078
DENAB/0.049 M HFIP			
13.93	0.300	16.30	0.322
14.71	0.316	17.13	0.243
15.39	0.287	18.11	0.218
DENAB/0.128 M MeOH			
11.49	0.185	14.38	0.088
11.85	0.133	14.68	0.087
12.32	0.089	15.14	0.082
12.62	0.095	15.63	0.074
12.94	0.088	16.18	0.067
13.31	0.096	16.78	0.061
13.50	0.090	17.55	0.057
13.79	0.092	18.47	0.047
13.96	0.087	19.01	0.042
DENAB/0.056 M DMA			
10.92	0.140	13.99	0.067
11.32	0.096	14.64	0.062
11.65	0.076	15.16	0.058
12.07	0.080	15.74	0.051
12.43	0.079	16.46	0.044
12.80	0.082	17.25	0.039
13.22	0.077	18.18	0.034
13.50	0.072	18.86	0.030

[a] The uncertainty of the data is ±5%.

TABLE 10: Rate Constants for Cis to Trans Thermal Relaxation of DENAB in SCF CO_2 45 °C[a]

density (mol/L)	*k* (1/s)	density (mol/L)	*k* (1/s)
8.474	0.178	11.06	0.102
8.97	0.102	11.69	0.092
9.52	0.084	11.98	0.099
10.21	0.124	12.55	0.087
10.55	0.111	13.00	0.075

[a] The uncertainty of the data is ±5%.

with increasing solvent density (shown in Figure 6 as a function of reduced density). The activation volume observed is positive, and relatively small for SCF reactions: $\Delta v^{\ddagger} = +170 \pm 225$ mL/mol for ethane and $+560 \pm 350$ mL/mol for CO_2.

The rate constants, even at the highest measured density (i.e., slowest rate), are approximately an order of magnitude greater than the corresponding rate constant in cyclohexane (0.0071 s^{-1}), even though the dielectric constant in the pure SCFs is smaller than that of cyclohexane.[1] The viscosity of cyclohexane is approximately an order of magnitude greater than that of the SCF solvents, and the rate constant varies inversely with solvent viscosity for thermal isomerization in both pure SCF CO_2 and ethane (illustrated when comparing Figure 7 to Figure 6).[43] It is tempting to attribute the solvent effects to viscosity, especially with a positive activation volume.

TABLE 11: Rate Constants for Cis to Trans Thermal Relaxation of DR in SCF CO_2 and Cosolvent-Modified Solvents at 35 °C[a]

density (mol/L)	*k* (1/s)	density (mol/L)	*k* (1/s)
DR/Pure CO_2			
14.09	0.100	16.07	0.081
15.05	0.082	17.03	0.071
15.63	0.084	17.69	0.066
DR/0.064 M MeOH			
14.36	0.134	15.75	0.091
14.65	0.093	16.52	0.089
15.16	0.100	17.32	0.077
15.45	0.091	18.24	0.071
DR/0.049 M HFIP			
13.53	0.346	17.12	0.183
14.43	0.305	17.82	0.165
15.26	0.284	18.76	0.132
16.34	0.199		

[a] The uncertainty of the data is ±5%.

TABLE 12: Rate Constants for Cis to Trans Thermal Relaxation of DMNAB in SCF CO_2[a]

density (mol/L)	*k* (1/s)	density (mol/L)	*k* (1/s)
12.55	0.101	15.11	0.060
13.00	0.076	16.08	0.044
13.51	0.069	17.08	0.038
14.31	0.064	18.05	0.031

[a] The uncertainty of the data is ±5%.

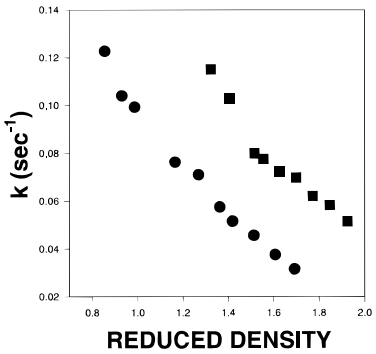

Figure 6. Rate constant vs reduced density for DENAB in SCFs CO_2 and ethane (●, CO_2, ■, ethane).

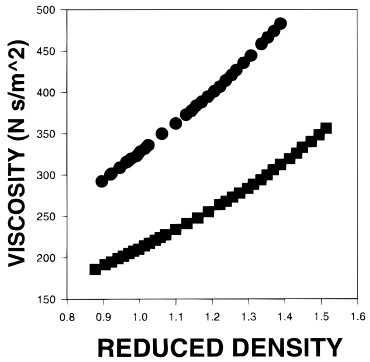

Figure 7. Viscosity as a function of reduced density for SCFs CO_2 and ethane (●, CO_2, ■, ethane).

Since the solvents are aprotic and the dielectric constant is low (1.2−1.5 in this region for both solvents), the reaction most likely proceeds via an inversion mechanism, which has not been reported to be viscosity dependent. While positive activation volumes in liquids can signal mass-transfer-limited reactions, the activation volume in SCFs is of little significance in determining mechanism. In liquids, structural and solvation

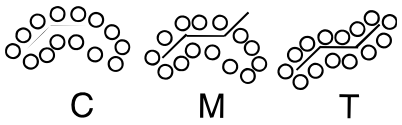

Figure 8. Schematic of two-step mechanism with solvent rearrangement.

contributions are roughly comparable in size, about ±30 cm^3/mol; in SCFs the structure contributions are presumably the same size, but they are virtually always overwhelmed by the solvation contributions, which can be hundreds of mL/mol or even L/mol. Thus, all the activation volume really tells us is that the difference of large numbers for solvation between transition state and substrate is positive by as little as only a few percent of their absolute values. Since the viscosity of SCFs is a strong function of their density, it seems consistent to consider the rates as density dependent.

The viscosity effect on unimolecular isomerization reactions in SCF solvents is relatively unexplored. The ratio of cis-/*trans*-stilbene was reported to be a strong function of SCF CO_2 viscosity in the near-critical region.[44] It is possible that this strong dependence on the solvent viscosity observed is actually due to the dependence of viscosity on solvent density. In this case, the trend of the ratio of cis-/*trans*-stilbene may be described as a function of density.

The viscosity effects on the thermal isomerization of DENAB were recently investigated by Sumi and co-workers[45] in methyl acetate and in two relatively viscous liquids, 2-methyl-2,4-pentanediol (MPT) and glycerol triacetate (GTA), where it was possible to vary the viscosity by many orders of magnitude by adjusting the pressure. In these two solvents, the rates initially increased with pressure due to normal transition state electrostriction of the solvent about the very polar (rotational) transition state. At a certain point, the viscosity becomes great enough that the rate begins to slow with additional pressure. However, viscosities many orders of magnitude higher than those in SCFs were required to see this effect.

We propose a mechanism similar to that developed by Sumi to explain the rate behavior observed in the SCF experiments:

$$\mathrm{C} \underset{k_{-1}}{\overset{k_1}{\rightleftharpoons}} \mathrm{M} \xrightarrow{k_2} \mathrm{T}$$

In this equation, C is the cis isomer with its equilibrium solvent shell and T is the trans isomer with its equilibrium solvent shell as shown in Figure 8. We view the intermediate configuration not as a transition state in the classical sense, but rather as the isomerized molecule before the concomitant rearrangement of the solvent shell. The first step is the structural change, where the energy barrier must be crossed by rapid atomic vibrations. The second step is the rearrangement of molecules to accommodate the new molecular species and is subject to a density dependence. In cases where the electrical environment does not change (solvent properties remain constant, isopolar transition state (polarities of C and M are constant), etc.) the changes in the rate constant are due to the changes in solvent density. This mechanism is strictly for the inversion process, while the rotation process is envisioned to proceed through a one-step mechanism.

This two-step mechanism can be illustrated by the following rate equation

$$\text{rate} = \frac{k_1 k_2}{k_{-1} + k_2}[\mathrm{C}]$$

In the case where $k_2 \gg k_{-1}$ the rate equation reduces to

$$\text{rate} = k_1[\mathrm{C}]$$

which indicates that the solvent shell reorganizes very rapidly and that the rate is kinetically controlled. In the case where k_{-1} (in the case of equilibrium $k_{-1} = k_1$) $\gg k_2$, the rate becomes

$$\text{rate} = \frac{k_1 k_2}{k_{-1}}[\mathrm{C}]$$

and the structural step occurs much faster than the solvent reorganization and the rate is then partially dependent on this rate of solvent reorganization. In this experiment, the solvent rearrangement step is believed to occur on a comparable or slower time scales than the reaction time. In this case, the rate of solvent rearrangement enters into the rate expression. In this case, at the lower solvent densities, where there are fewer solvent molecules, the rate increases due to increases in k_2.

The ability to "tune" the reaction rate of this thermal relaxation by over 4 times in a very limited density region of SCF CO_2 is remarkable. In a single solvent, the reaction rate is tuned to an extent that could only be achieved by changing from liquid solvents with increasing polarities. This experiment demonstrates that solvent density is a very important tunable property for isomerization reactions, as well as other unimolecular reactions, in near-critical SCF solvents. Opportunities exist for further tunability of the reaction rate with small additions of cosolvents, due to local composition enhancements near the critical point of the system.

Cosolvent Modified Experiments. The thermal cis−trans relaxation kinetics for DENAB, primarily, and DR were measured in SCF CO_2 and ethane with small amounts of acetone, DMA, methanol, and HFIP cosolvents.[46] The concentrations and mole fraction ranges for the added cosolvents are shown in Table 6. The experiments were carried out in constant *concentration* of cosolvent. The mole fraction changed as SCF was added throughout each experiment. The composition may be enhanced in the near-critical region where local composition of cosolvent about the solute (i.e., reactant) may be several times the bulk composition.[32,47−53] By using cosolvents with varying degrees of acidity, basicity (HBD or HBA ability, in this case), and polarity/polarizability, it is possible to analyze the effect of these specific solvent properties while maintaining bulk solvent properties much like that of the pure SCF fluid. In liquid studies, high polarity/polarizability cannot be easily separated from specific interactions because most acid or basic (HBD or HBA) solvents also have large dielectric constants or Kamlet−Taft polarity/polarizability parameters. This is more readily accomplished in SCF/cosolvent media.

The cosolvent experiments revealed the following key points: (1) small amounts of polar or protic cosolvents are capable of tuning the reaction rate many times over that in the pure SCF solvent; (2) rapid increases in the rate constant in the near-critical region may be due to local composition enhancements of cosolvent about the reactant; (3) polar, aprotic cosolvents modestly enhance the reaction rate; (4) protic cosolvents, regardless of polarity, enhance reaction rate dramatically; (5) the data are consistent with a change in mechanism to rotation in the presence of protic cosolvents.

Each of these points will be discussed in detail below with specific experimental results to serve as examples for each key point.

When aprotic, polar cosolvents such as acetone and DMA are added to SCF ethane and CO_2, the rate of thermal cis−

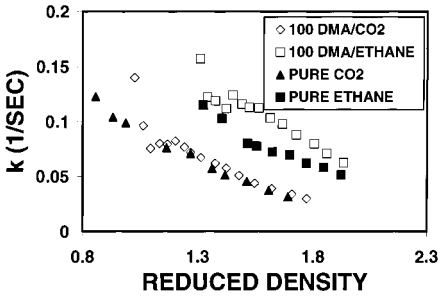

Figure 9. First-order rate constants for the thermal cis−trans isomerization of DENAB with cosolvent DMA as a function of reduced density.

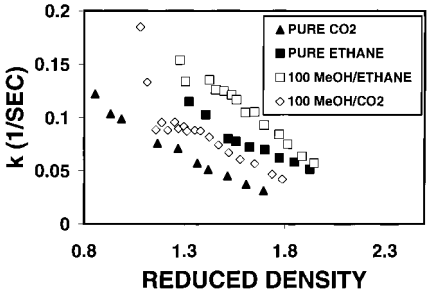

Figure 10. First-order rate constants for the thermal cis−trans isomerization of DENAB with cosolvent MeOH as a function of reduced density.

trans isomerization of DENAB is very close to that in the pure SCFs until the near-critical region is approached (Figure 9). Cosolvent DMA enhances the rate in ethane slightly more than in CO_2 at the same reduced densities, perhaps because of the lack of specific interactions between the ethane and DMA, which may strengthen the interactions between the polar solute molecule and the cosolvent. In both solvents, in the very near-critical region, we suggest that local composition enhancements cause a disproportional increase in the local concentration of the cosolvent about the DENAB in relation to the bulk concentration, giving marked increases in the rate constant.

These trends with respect to pressure (or density) are consistent with the two-step rate hypothesis above. In the case of cosolvent/SCF solvents, the rate is always greater than that in the pure SCF. Here, the change in rate due to the density effect (solvent rearrangement) is similar to that in the pure SCF; however, the increased dielectric constant of the media resulting from the addition of the polar cosolvent causes an increase in the reaction rate (i.e., an increase in the structural rate constant, k_1).

In experiments involving the isomerization of DENAB in SCF CO_2 and ethane modified with methanol, similar results are found for DMA and acetone (see Figure 10). With MeOH cosolvent, the rate enhancements, as compared to the pure SCF solvents, are greater at all reduced densities than with the DMA or acetone, probably due to the ability of MeOH to hydrogen bond weakly to the nitro group of DENAB that enhances this group's electron withdrawing capability. The same result was found for DR.

The experiments with HFIP cosolvent were very difficult to analyze at the high cosolvent concentrations with non-flash photolytic analysis methods because of the extreme enhancements of the isomerization rate of both DENAB and DR. In Figure 11 the rate constants for DENAB and DR in HFIP modified SCF CO_2 are shown. In the case of pure DR, the lower pressure limit for the data is high because of the low solubility of DR in pure CO_2; however, for DR and DENAB

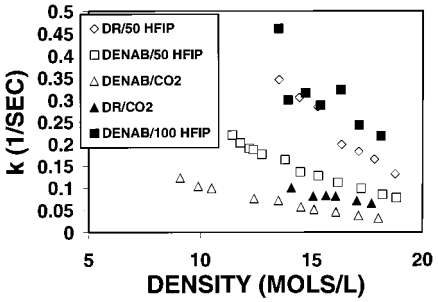

Figure 11. First-order rate constants for the thermal cis−trans isomerization of DENAB and DR with cosolvent HFIP in SCF CO_2 as a function of density.

with 0.05 M HIFP, the data are limited because the rate constants were so large (fast) that they could not be accurately measured at lower pressures. In addition, there was a much smaller percent of cis isomer present at the photostationary state. However, the rate was found to increase over 15 times with the addition of less than 0.4 mol % HFIP. This rate enhancement is truly remarkable for such a small amount of added cosolvent; it can be explained only by strong specific interactions of the hydrogen-bonded cosolvent to the nitro group of the solute molecules, going through a highly dipolar transition state (associated with a rotation mechanism). The bulk dielectric constant will remain very similar to that of SCF CO_2 at these concentrations, while the local dielectric may be several times greater in the near-critical region due to local composition enhancements—this would lead to a local dielectric which is still relatively low. In fact, the dielectric environment would be lower than in the previous DMA, acetone, and methanol experiments. Therefore, with no change mechanism (i.e., a reaction proceeding by inversion), the reaction rate would be expected to be similar to or lower than the previous experiments. However, HFIP has a very large acidity parameter ($\alpha = 1.96$) and no basic nature whatsoever (unlike the case of methanol, which is a weak HBD and strong HBA molecule) and is capable of strong hydrogen bonding interactions with the reactant.

Whitten and co-workers[1] noted that in a correlation of rate constants for the thermal isomerization of DENAB with the Kosower parameter for 14 protic and aprotic solvents that the plot broke up into two distinct linear regions for the protic and aprotic solvents. This was attributed to the lowering of the energy barrier of isomerization when the solvent interacts specifically with the solute via the nitro group, thus enhancing its ability to withdraw electrons. Our experimental data provides additional evidence for the lowering of the energy barrier via specific hydrogen bond interactions with the nitro group.

A Kirkwood analysis was performed and was consistent with the above hypothesis. The existence of local composition enhancements in the near-critical region results in a need for a "local" dielectric constant to be calculated for the analysis. Kim and Johnston[54] determined local composition enhancements for several cosolvents in SCF CO_2 as a function of pressure and cosolvent composition spectroscopically by measuring the transition energy of the solvatochromic dye, phenol blue. We have used these data, which reveal local composition enhancements up to 7.5 times that of the bulk composition at reduced pressures of just over unity, to estimate "local" dielectric constants for the CO_2/methanol systems. Local dielectric constants were calculated for the ethane/CO_2 system using local composition enhancement data from a separate experiment.[55] Because the reactant used in this investigation is not identical to the probe molecules used in these determinations of local composition enhancement, this is only an estimation. The fluid

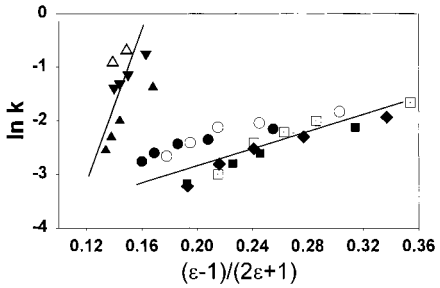

Figure 12. Kirkwood plot for DENAB in SCF CO_2 and SCF ethane modified with cosolvents: ■, methanol−CO_2; ▲, HFIP−CO_2, low concentration; ▼, HFIP−CO_2, high concentration; ◆, DMA−CO_2; ●, acetone−ethane; □, methanol−ethane; ○, DMA−ethane; △, HFIP−ethane.

was treated as having finite spaces about the central solute, and the local dielectric was calculated by a linear sum of the contributions from the supercritical fluid and the cosolvent.

The Kirkwood plot for DENAB in SCF CO_2 with 0.128 M MeOH using the "local" dielectric constant (Figure 12) shows a linear relationship, indicating that the sharp rate increase in the near-critical region may be due to an enhanced dielectric environment arising from local composition enhancements of cosolvent about DENAB in this region. However, the "local" dielectric constant never exceeds ∼4 in the region with greatest local composition enhancements, so the mechanism of isomerization should remain dominantly inversion. For this reason, no deviations in the Kirkwood plot occur.

However, the Kirkwood plot for DENAB in SCF CO_2 with 0.025 M HFIP indicates that at much lower dielectric values, the reaction rate is much faster than for the more strongly dielectric cosolvents: methanol, acetone, and DMA. The positive deviations in the Kirkwood plot occur in the near-critical region as the local composition of HFIP becomes great enough for the rotation mechanism to become competitive with the inversion mechanism. Even at the lowest density, where local composition enhancements are greatest, the local dielectric was estimated to be ∼2.5. This supports the supposition that the mechanism must no longer be inversion. The strong acidity of this cosolvent results in a very dipolar transition state that likely proceeds via the rotation mechanism. The positive deviations of the HFIP data from the Kirkwood plots provide additional evidence that the strong protic solvents cause a change in mechanism from inversion to rotation and allow the effects of dielectric and HBD solvents to finally be separated.

Conclusions

From this work it was found that there is a several-fold solvent effect on the rate of thermal isomerization of push−pull azobenzenes in pure SCFs. The variation in rate constant with density correlates with the density of the solvent for pure SCF ethane and CO_2; a mechanism consistent with the data is proposed.

It has been shown that with less than 0.5 mol % cosolvent, the reaction rate may vary more than 15-fold. This tremendous rate enhancement is the result of a combination of local composition enhancements, which provide an enriched dielectric environment about the solute, and specific interactions, which lower the energy barrier of reaction. This work demonstrates the ability of strong hydrogen bond donating solvents to change the mechanism while dielectric environment remains low. From the experimental data we have shown that reaction rates can be tuned substantially with very low concentrations of cosolvents due to an enriched dielectric environment in the near-critical region. It seems clear that extreme rate enhancements occur due to strong specific hydrogen bond interactions of protic cosolvents with the nitro group of the solutes which result in a change in mechanism from inversion to rotation.

These results also show the tremendous potential for SCFs as reaction solvents; very often they provide environmentally benign alternatives to undesirable liquid solvents, and they permit precise tuning not only of rates, but also of yields or product distributions[55−57]

Acknowledgment. The authors are grateful for the financial support of the National Science Foundation and of the DuPont Co.

Notation

k = rate constant (s^{-1})

Greek Letters

α = Kamlet−Taft acidity parameter
β = Kamlet−Taft basicity parameter
$\Delta G^{\ddagger}$ = Gibbs energy of activation
$\Delta V^{\ddagger}$ = activation volume
ϵ = dielectric constant
π^* = Kamlet−Taft polarity/polarizability parameter

References and Notes

(1) Schanze, K. S.; Mattox, T. F.; Whitten, D. G. *J. Org. Chem.* **1983**, *48*, 2808−2813.
(2) Hartley, G. S. *J. Chem. Soc.* **1938**, 633−642.
(3) Cataliotti, R. S.; Morresi, A.; Paliani, G.; Zgierski, M. Z. *J. Raman Spectrosc.* **1989**, *20*, 601−604.
(4) Liu, Z.-F.; Morigaki, K.; Enomoto, T.; Hashimoto, K.; Fujishima, A. *J. Phys. Chem.* **1992**, *96*, 1875−1880.
(5) Barrett, C.; Natansohn, A.; Rochon, P. *Chem. Mater.* **1995**, *7*, 899−903.
(6) Barret, C.; Natansohn, A.; Rochon, P. *Macromolecules* **1994**, *27*, 4781−4786.
(7) Rau, H. In *Photochemistry and Photophysics*; Rabek, J. F., Ed.; CRC Press: Boca Raton, FL, 1990.
(8) Asano, T.; Okada, T. *J. Org. Chem.* **1984**, *49*, 4387−4391.
(9) Asano, T.; Yano, T.; Okada, T. *J. Am. Chem. Soc.* **1982**, *104*, 4900−4904.
(10) Andersson, J.-A.; Petterson, R.; Tegner, L. *J. Photochem.* **1982**, 17−32.
(11) Otruba, J. P.; Weiss, R. G. *J. Org. Chem.* **1983**, *48*, 3448−3453.
(12) Nishimura, N.; Tanaka, T.; Asano, M.; Sueishi, Y. *J. Chem. Soc., Perkin. Trans. 2* **1986**, 1839−1845.
(13) Marcandalli, B.; Pellicciari-Di Liddo, L.; Di Fede, C.; Bellobono, I R. *J. Chem. Soc., Perkin. Trans. 2* **1984**, 589−593.
(14) Nishimura, N.; Kosako, S.; Sueishi, Y. *Bull. Chem. Soc. Jpn.* **1984**, *57*, 1617−1625.
(15) Sanchez, A. M.; de Rossi, R. H. *J. Org. Chem.* **1995**, *60*, 2974−2976.
(16) Schanze, K. S.; Mattox, T. P.; Whitten, D. G. *J. Am. Chem. Soc.* **1982**, *104*, 1733−1735.
(17) Nerbonne, J. M.; Weiss, R. G. *J. Am. Chem. Soc.* **1978**, *100*, 5953.
(18) Wildes, P. D.; Pacifici, J. G.; Irick, G. I., Jr.; Whitten, D. G. *J. Am. Chem. Soc.* **1971**, *93*, 2004−2008.
(19) Sigman, M. E.; Leffler, J. E. *J. Org. Chem.* **1987**, *52*, 3123−3126.
(20) McHugh, M.; Krukonis, V. *Supercritical Fluid Extraction*, 2nd ed.; Buttersworth-Heinemann: Boston, MA, 1994.
(21) Kazarian, S. G.; Poliakoff, M *J. Phys. Chem.* **1995**, *99*, 8624.
(22) Kazarian, S. G.; Gupta; R. B.; Clarke, M. J.; Johnston, K. P.; Poliakoff, M. *J. Am. Chem. Soc.* **1993**, *115*, 11099.
(23) Gurdial, G.; Macnaughton, S. J.; Tomasko, D. L.; Foster, N. R *Ind. Eng. Chem. Res.* **1993**, *32*, 1488−1497.
(24) Ting, S. S. T.; Tomasko, D. L.; Foster, N. R. *Ind. Eng. Chem. Res.* **1993**, *32*, 1471−1481.
(25) Eckert, C. A.; Knutson, B. L. *Fluid Phase Equilib.* **1993**, *83*, 93−100.
(26) Ekart, M. P.; Bennett, K. L.; Ekart, S. M.; Gurdial, G. S.; Liotta, C. L.; Eckert, C. A. *AIChE J.* **1993**, *39*, 235−248.
(27) Tomasko, D. L.; Knutson, B. L.; Pouillot, F. L. L.; Liotta, C. L.; Eckert, C. A. *J. Phys. Chem.* **1993**, *97*, 11823−11834.

(28) Dillow, A. K.; Yun, S. L. J.; Sueliman, D.; Boatright, D.; Liotta, C. L., Eckert, C. A. *Ind. Eng. Chem. Res.* **1996**, *35*, 1801−1806.

(29) Dillow, A. K. Investigations of Reactions in Supercritical Fluids and Applications to Environmental Processing. Ph.D. Thesis, Department of Chemical Engineering, Georgia Institute of Technology, 1996.

(30) Rhodes, T. A.; O′Shea, K. O.; Bennett, G.; Johnston, K. P.; Fox, M. A. *J. Phys. Chem.* **1995**, *99*, 9903−9908.

(31) Savage, P. E.; Gopalan, S.; Mizan, T. I.; Martino, C. J.; Brock, E. E. *AIChE J.* **1995**, *41*, 1723−1778.

(32) Knutson, B. L.; Dillow, A. K.; Liotta, C. A.; Eckert, C. A. In *Innovations in Supercritical Fluids: Science and Technology*; Hutchenson, K. W., Foster, N. R., Eds.; American Chemical Society: Washington, DC, 1995.

(33) Ellington, J. B.; Park, K. M.; Brennecke, J. F. *Ind. Eng. Chem. Res.* **1994**, *33*, 965−974.

(34) Roberts, C. B.; Chateauneuf, J. E.; Brennecke, J. F. *J. Am. Chem. Soc.* **1992**, *114*, 8455−8463.

(35) Randolph, T. W.; Carlier, C. *J. Phys. Chem.* **1992**, *96*, 5146−5151.

(36) Kazarian, S. G.; Vincent, M. F.; Bright, F. V.; Liotta, C. L.; Eckert, C. A. *J. Am. Chem. Soc.* **1996**, *118*, 1729.

(37) Kazarian, S. G.; Vincent, M. F.; Eckert, C. A. *Rev. Sci. Instrum.* **1996**, *67*, 1586.

(38) Yun, S. L. J.; Dillow, A. K.; Eckert, C. A. *J. Chem. Eng. Data* **1996**, *41*, 791−793.

(39) Foster, N. R.; Singh, H.; Yun, S. L. J.; Tomasko, D. L.; Macnaughton, S. J. *Ind. Eng. Chem. Res.* **1993**, *31*, 2849−2853.

(40) Gurdial, G. S.; Foster, N. R. *ACS Symp. Ser.* **1992**, *514*, 34−45.

(41) Hafner, K. P. Ph.D. Thesis, Georgia Institute of Technology, 1996.

(42) Peng, D. Y.; Robinson, D. B. *Ind. Eng. Chem. Fundam.* **1976**, *15*, 59.

(43) Iwasaki, H.; Takahashi, M. *J. Chem. Phys.* **1981**, *74*, 1930−1943.

(44) Squires, T. G.; Venier, C. G.; Aida, T. *J. Fluid Phase Equilib.* **1983**, *10*, 261−268.

(45) Asano, T.; Cosstick, K.; Furuta, H.; Matsuo, K.; Sumi, H. *Bull. Chem. Soc. Jpn.* **1996**, *69*, 551−560.

(46) Experimental rates were also obtained for DENAB in SCF CO_2 and ethane with chloroform cosolvent. However, the replicate rate measurements in these circumstances varied substantially and it is believed that unknown complications in the reaction mechanism exist. Therefore, we have not included the chloroform cosolvent data at this time.

(47) Phillips, D. J.; Brennecke, J. F. *Ind. Eng. Chem. Res.* **1993**, *32*, 943−951.

(48) O'Brien, J. A.; Randolph, T. A. *AIChE J.* **1993**, *39*, 1061−1071.

(49) Sun, Y.; Fox, M. A.; Johnston, K. P. *J. Am. Chem. Soc.* **1992**, *114*, 1187−1194.

(50) Brennecke, J. F.; Tomasko, D. L.; Eckert, C. A. *J. Phys. Chem.* **1990**, *94*, 7692−7700.

(51) Wu, R. S.; Lee, L. L.; Cochran, H. D. *Ind. Eng. Chem. Res.* **1990**, *29*, 977−988.

(52) Petsche, I. B.; Debenedetti, P. G. *J. Phys. Chem.* **1989**, *9*, 7075−7084.

(53) Yonker, C. R.; Smith, R. D. *J. Phys. Chem.* **1988**, *92*, 2374−2378.

(54) Kim, S.; Johnston, K. P. *AIChE J.* **1987**, *33*, 1603−1611.

(55) Dillow, A. K.; Hafner, K. P.; Yun, S. L. J.; Feng, F.; Kazarian, S. G.; Liotta, C. L.; Eckert, C. A. *AIChE J.* **1997**, *43*, 515−524.

(56) Eckert, C. A.; Knutson, B. L.; Debenedetti, P. G. *Nature*, **1996** *383*, 313−318.

(57) Eckert, C. A.; Chandler, K. Tuning of Solvents for Chemical Reactions. Presented at the 4th Meeting on Supercritical Fluids, Sendai, Japan, May 1997.

(58) Kamlet, M. J.; Abboud, J.-L., M..; Abraham, M. H.; Taft, R. W. *J. Org. Chem.* **1983**, *48*, 2877−2887.

(59) Murto, J.; Kivinen, A.; Lindell, E. *Sumomen Kiemistiehiti B* **1970**, *43*, 28−30.

(60) Everson, R. C.; van der Merwe, B. J. *Fluid Phase Equilib.* **1998**, *143*, 173−184.

(61) Reid, R. C.; Prausnitz, J. M.; Poling, B. E. *The Properties of Gases and Liquids*; McGraw-Hill: New York, 1987.

(62) For HFIP and DMA the critical temperature and pressure were calculated from Joback method; acentric factor was calculated by Lee−Kesler method, found in ref 56.